

STABILITY OF IRON IN CLAYS UNDER DIFFERENT LEACHING CONDITIONS

BARBORA DOUSOVA^{1,*}, LUCIE FUITOVA¹, DAVID KOLOUSEK¹, MILOSLAV LHOTKA¹, TOMAS MATYS GRYGAR²,
AND PETRA SPURNA¹

¹ Institute of Chemical Technology in Prague, Technická 5, 166 28 Prague 6, Czech Republic

² Institute of Inorganic Chemistry AS CR, 250 68 Řež, Czech Republic

Abstract—The iron chemistry of aluminosilicates can markedly affect their adsorption properties due to possible changes in surface charge upon exposure to a variety of processes in the environment. One of these processes is chemical leaching, but to date little has been reported on the susceptibility of structural Fe to chemical leaching. The purpose of the current study was to determine the effects of solution pH on the stability of structural Fe in kaolinites, illite, and bentonite and the potential for formation of ancillary (oxyhydr)oxides. Structurally bound Fe does not participate in sorption properties but Fe that is released and phase transformed during leaching could take part in adsorption processes and form complexes and/or covalent bonds *via* Fe ions. Five different Fe-bearing clay minerals were treated in 0.5 M and 2 M HCl, distilled H₂O, 0.1 M KCl, and 0.5 M KHCO₃ for 24 h. The amount of Fe leached varied from 10 μg g⁻¹ (for 0.1 M KCl) to 10⁴ μg g⁻¹ (for 2 M HCl) depending on the leaching agents. Acidic and water treatments indicated a relative independence of leached Fe on the initial Fe content in the clay and, conversely, a heavy dependence on the crystallinity of initial Fe phases. Well crystallized Fe(III) was stable during the leaching process, while poorly crystallized and amorphous Fe(III) phases were less stable, forming new ion-exchangeable Fe³⁺ particles. Under alkaline conditions, no relation between Fe crystallinity and mobility was found. The structural and surface changes resulting from leaching processes were identified by equilibrium adsorption isotherms. In kaolinite, the specific surface area (*S*_{BET}) and porosity changed independently of Fe leaching due to the stability and crystallinity of Fe. In bentonite, the number of micropores was reduced by their partial saturation with Fe³⁺ particles caused by poorly crystallized and more reactive Fe forms during the leaching process. Potential phase transformations of Fe were characterized by the voltammetry of microparticles; well crystallized Fe(III) oxides remained stable under leaching conditions, while poorly crystallized and amorphous Fe(III) phases were partially dissolved and transformed to reactive Fe³⁺ forms.

Key Words—Clays, Iron, Leaching Stability, Structure, Surface Properties.

INTRODUCTION

Iron chemistry controls most surface and subsurface geochemical processes due to the variability of Fe species, their widespread occurrence, pH/Eh sensitivity, and, initially, a high sorption affinity in the solid–liquid interface. Iron cations in the two main structural groups of clay minerals mostly occupy the octahedral sheets (Stucki *et al.*, 1988); their form and oxidation states vary according to the mineralogical and environmental conditions. In kaolinites, most Fe is present in the structure; some has been identified as the Fe(II) form (Bonin *et al.*, 1982, Hassan and Salem, 2002). Free oxides and hydroxides have also been recognized as discrete particles or as coatings bound to the particle surface, typically at the rate of ~0.5 g of Fe₂O₃/kg of kaolin (Ferris and Jepson, 1975). Most 2:1 clay minerals contain some structural iron in the octahedral sheets, both in the Fe(II) and Fe(III) forms (Stucki *et al.*, 1988). Structural Fe provides a significantly greater binding stability than surface Fe phases (Ferris and Jepson, 1975). The equilibrium between Fe³⁺ and Fe²⁺ particles

in layer silicates can be considered responsible for important physical-chemical properties of these materials (Favre *et al.*, 2006; Komadel *et al.*, 2006; Manceau *et al.*, 2000).

The chemical and/or bacterial reduction of structural Fe also modifies some properties (Pentráková *et al.*, 2013), including the layer charge and the cation exchange capacity (CEC), which are closely related to adsorption/desorption processes on the surface. In natural environments, especially in soils, structural Fe in clay minerals and Fe (oxyhydr)oxides (usually denoted as HFO) coexist (Favre *et al.*, 2006) and can be present as individual particles; most commonly, they form stable organomineral species or HFO-coated particles. Though the presence of Fe (oxyhydr)oxides in relation to clay minerals can contribute significantly to their sorption properties, little evidence of the transformation of structurally bound Fe to a surface-coating of hydrated Fe³⁺ particles has been found (Sei *et al.*, 2002).

Over the past ten years, surface modification of aluminosilicates with Fe ions has opened up new possibilities in adsorption technologies due to the change in the surface charge (pH_{ZPC}) of aluminosilicates and, thus, a strong affinity for anionic contaminants (Doušová *et al.*, 2009; Izumi *et al.*, 2005). Through the

* E-mail address of corresponding author:

Barbora.Dousova@vscht.cz

DOI: 10.1346/CCMN.2014.0620207

interaction of raw clay mineral and Fe-salt solution, reactive ion-exchangeable forms of amorphous and/or poorly crystalline HFO particles in a stable oxidation state, Fe(III), are fixed on the clay-mineral surface forming active adsorption sites. The considerable variability in growing Fe phases (hydrated Fe₂O₃, non-specific Fe³⁺ particles, ferrihydrite) resulted from the different types of minerals and the treatment conditions (Doušová *et al.*, 2009). According to Burleson and Penn (2006), most of the newly created active sites can subsequently be fixed in surface complexes during adsorption processes, while unoccupied sites tend to be transformed to more stable and/or crystalline mineral Fe phases (*e.g.* goethite).

The above-described processes also take place in the natural environment (Dávila-Jiménez, 2008). Even dissolved Fe ions can participate *in situ* in adsorption/desorption processes; during co-adsorption, hydrated Fe particles are bound preferentially to active sites due to their excellent sorption affinity for clay mineral surfaces. Reactive Fe(II/III) particles form new active sorption sites which mostly attract anionic particles from aqueous systems (Doušová *et al.*, 2011; Yang *et al.*, 2007).

Generally, a surface-fixed and/or structurally bound Fe affects the surface properties of clay minerals (adsorption/desorption, transformation of particles to more or less stable forms, and mobility of surface-fixed particles, depending on pH/Eh changes). The main aim of the present study was, therefore, to determine the stability of Fe in selected types of clay minerals under various chemical leaching conditions; specifically, to measure the effects of changes in structural Fe content on the clay-mineral structure and crystallinity and to correlate such changes with the initial iron content and the leaching agent used.

MATERIALS AND METHODS

Clays with large bound-Fe contents

Five different types of Fe-rich clays were studied: kaolinite from Király Hill in Hungary (KH); illite from

an illite pit in Tokai, Hungary (IH); smectite known as 'Red Clay' from a lignite pit in Visonta, Hungary (RCH); kaolinite from a clay deposit in West Bohemia, Czech Republic (KCR); and bentonite with a large smectite content from a bentonite pit in West Bohemia, Czech Republic (BCR). These materials were washed with distilled water, dried at 60°C, homogenized using a mortar and pestle, and finally sieved to 0.355 mm.

The main chemical and mineralogical characteristics of the clays used are summarized in Table 1.

Leaching agents

For leaching experiments, five different solutions or leaching agents were used: (a) 0.5 M HCl (pH = 1.1), (b) 2.0 M HCl (pH = 0.7), (c) 0.1 M KCl (pH = 6.3), (d) 0.5 M KHCO₃ (pH = 8.3), and (e) H₂O (pH = 5.6). The solutions were prepared from chemicals of analytical-reagent grade (Merck, Penta, Czech Republic) and distilled water at ambient temperature (25°C).

Leaching procedure

Experiments were run in a batch manner at a solid:liquid ratio of 1:10, laboratory temperature (20°C), and leaching times of 1 h, 2 h, 5 h, 8 h, and 24 h. The leaching products were separated by filtration; the filtrate was analyzed for residual Fe content, while the solid part was tested using the methods described below (*S*_{BET} and pore distribution, voltammetry of microparticles).

Analytical methods

The concentration of Fe_{tot} in aqueous solutions was measured with a UV/VIS spectrophotometer (UNICAM 5625, Richmond Scientific, Ltd., Lancashire, UK) using the Fe³⁺ chelate complex method (with EDTA) at 520 nm (Malat, 1973).

The amount of Fe(II) present in the clay minerals was determined by the manganometric titration method (Alvarez Querol, 1952); 200 mg of solid sample was exposed to a mixture of acids (10 mL of 10% H₂SO₄ and 5% H₃PO₄), distilled water (30 mL), and (NH₄)₂SO₄ (100 mg) under an inert atmosphere (N₂) for 20 min. The

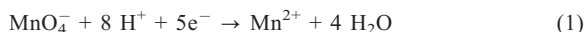
Table 1. Mineralogical and chemical properties of the clays used in the present study.

Sample	Fe _{tot} (mg g ⁻¹)	Fe ²⁺ (mg g ⁻¹)	Mineralogical composition	Fe crystallinity*
KH	21.3	10.4	kaolinite, quartz, pyroxene	Very high (~90%)
IH	12.2	1.0	illite, quartz, goethite	High (>60%)
RCH	48.0	6.4	montmorillonite, quartz, kaolinite, hematite	Low (~20%)
KCR	62.4	12.5	montmorillonite, illite, kaolinite, quartz	Moderate (50%)
BCR	106.4	1.3	montmorillonite, kaolinite, quartz, K-feldspar	Moderate (~30%) nanocrystals

KH: kaolinite from Király Hill, Hungary; IH: illite from a pit in Tokai, Hungary; RCH: smectite known as 'Red Clay' from a lignite pit in Visonta, Hungary; KCR: kaolinite from a clay deposit in west Bohemia, Czech Republic; BCR: bentonite with a large smectite content from a bentonite pit in west Bohemia, Czech Republic.

* determined by Mössbauer spectroscopy

suspension was titrated quickly with 0.02 M KMnO_4 to the end point, as given by reaction 1.



X-ray diffraction (XRD) of powder samples was done using a Seifert XRD 3000P diffractometer (Seifert, Ahrensburg, Germany) with $\text{CoK}\alpha$ radiation ($\lambda = 0.179026$ nm, graphite monochromator, goniometer with Bragg-Brentano geometry) over the range $5-60^\circ 2\theta$, step size $0.05^\circ 2\theta$.

X-ray fluorescence (XRF) analyses of the solid phase were done using an ARL 9400 XP+ spectrometer (ARL, Ecublens, Switzerland); voltage 20–60 kV, probe current 40–80 mA; effective area 490.6 mm^2 . *UniQuant* software was used to evaluate the data (Thermo ARL, Switzerland).

Transmission ^{57}Fe Mössbauer spectra were collected in constant acceleration mode using a $^{57}\text{Co}(\text{Rh})$ source (1.85 GBq). Powdered samples were prepared as conventional absorbers ($\sim 5 \text{ mg Fe cm}^{-2}$) and measured at room temperature and 25 K. The isomer shift (δ) was calibrated against an $\alpha\text{-Fe}$ foil at room temperature. Spectra were folded and fitted by Lorentz functions using the program *CONFIT2000* (Žák and Jirásková, 2006). The proportions of Fe phases were determined from the integral area of absorption subspectra.

Equilibrium adsorption isotherms of nitrogen were measured at 77 K using a static volumetric adsorption system (ASAP 2020 analyzer, Micromeritics, Norcross, USA), using samples leached for 24 h. The adsorption isotherms were fitted using the Brunauer-Emmett-Teller (BET) method for specific surface area (Brunauer *et al.*, 1938), the micropore volume by the t-plot method (Webb and Orr, 1997), and the pore-size distribution by the Barrett-Joyner-Halenda (BJH) method (Barrett *et al.*, 1951).

Voltammetry of microparticles was performed using a conventional paraffin-impregnated graphite electrode in a 1:1 acetate buffer with total acetate concentration of 0.2 M in linear sweep mode from open circuit potential in the negative direction at a scan rate of 3 mV/s (Grygar *et al.*, 2002). The potentials are given with respect to a saturated calomel reference electrode (SCE) and interpreted through comparison with the peak potentials, E_p , of reference oxides (Grygar *et al.*, 2002), free Fe^{3+} ions,

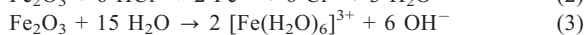
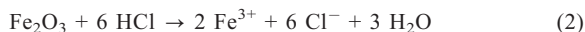
and oligomeric Fe(III) hydroxo-oxide species (Grygar *et al.*, 2007).

The parameters of Fe leaching were calculated according to first- and second-order kinetics (Sultana *et al.*, 2014). The reproducibility of leaching experiments was checked by parallel measurements; the standard deviation, which resulted from 10 experimental sets, did not exceed 7%.

RESULTS AND DISCUSSION

Stability of Fe under different leaching conditions

The rate and extent of dissolution of clay minerals is generally influenced by the mineral type, layer structure, and chemical composition (Madejová *et al.*, 2009). The reactions governing leaching in acid or water were, respectively:



The maximum amount of Fe ($\mu\text{g g}^{-1}$) leached from the samples in different environments at equilibrium are given in Table 2. Measurements of the release of Fe (Figure 1) revealed that the amount of Fe leached varied from $\sim 10 \mu\text{g}$ for 0.1 M KCl to $\sim 10^4 \mu\text{g}$ for 2 M HCl (Table 2).

Kinetics data (Table 3) for acidic leaching of BCR and KCR, which have the largest amounts of total Fe and moderate Fe crystallinity (see Table 1), were evaluated in light of reaction 2, which depended on the concentration of hydrogen ions according to a first-order rate equation. At increasing concentration of hydrogen ions, the rate of reaction increased. In the case of water leaching (reaction 3), second-order kinetics was involved because of a complex reaction mechanism with hydrolyzed products which resulted in a significantly slower reaction rate.

Regardless of the total Fe content, the stability of structural Fe in the clay minerals decreased in the following order for the respective leaching agents (a–e; Table 2):

acidic, a,b: KH > IH > KCR > RCH > BCR
 water, e: KH > IH \approx RCH > KCR > BCR
 alkaline, d: KCR \approx RCH > KH > BCR
 greater ionic strength, c: KH \approx IH > BCR > RCH > KCR

Table 2. Fe released from the clay minerals ($\mu\text{g g}^{-1}$) and the corresponding percentage decline in structural Fe_{tot} (%).

Sample	0.5 M HCl (a)	%	2 M HCl (b)	%	0.5 M KHCO_3 (d)	%	H_2O (e)	%	0.1 M KCl (c)	%
KH	156	0.7	986	4.6	29.2	0.1	17.8	0.08	17.7	0.1
IH	161	1.3	647	5.3			61.2	0.5	18.34	0.2
RCH	3085	6.4	7499	15.6	20.8	0.04	50.0	0.1	29.9	0.1
KCR	1731	2.8	5221	8.4	22.3	0.03	100.1	0.2	39.6	0.1
BCR	7500	7.1	23476	22.1	33.3	0.03	200.0	0.2	20.0	0.02

Sample names as in Table 1.

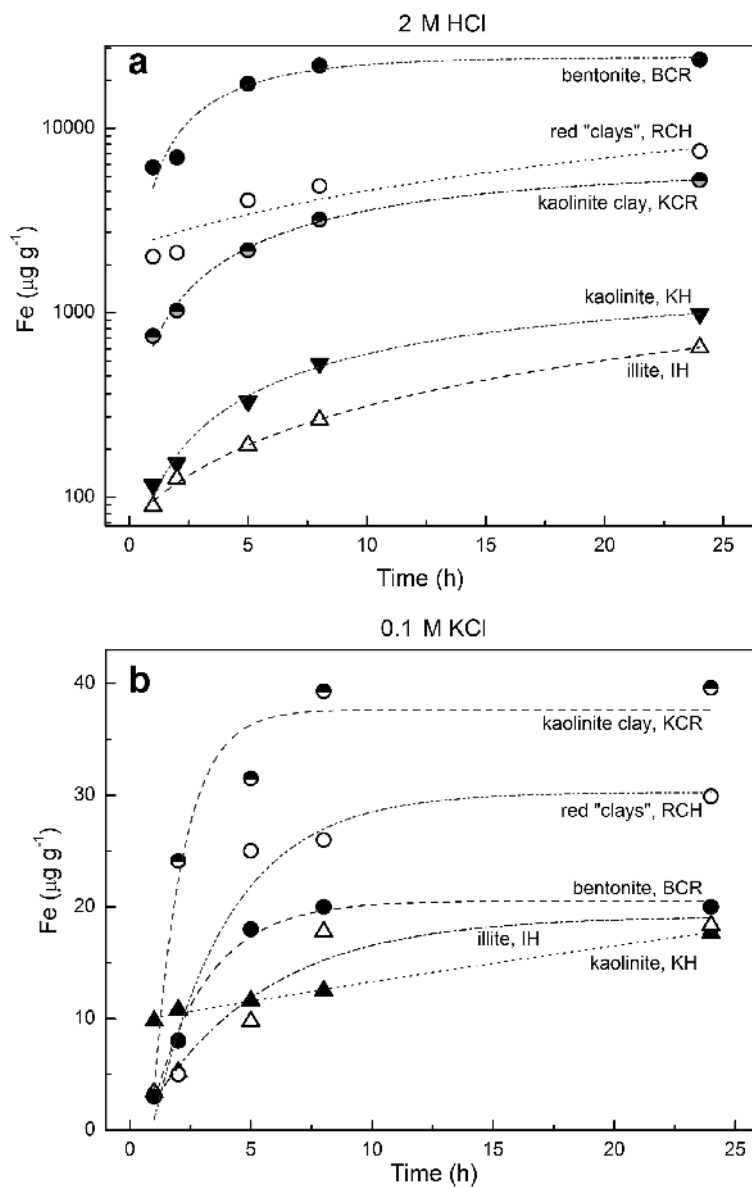


Figure 1. Time dependence of Fe release from clays during leaching processes: (a) 2 M HCl, (b) 0.1 M KCl.

Table 3. Kinetic data for acidic and water leaching.

Leaching agent	Kaolinite clay, KCR				Bentonite, BCR			
	Order	R^2	k^1 (h^{-1})	k^2 ($\text{g } \mu\text{g}^{-1} \text{h}^{-1}$)	Reaction order	R^2	k^1 (h^{-1})	k^2 ($\text{g } \mu\text{g}^{-1} \text{h}^{-1}$)
0.5 M HCl (1)	1 st	0.995	0.046	—	1 st	0.987	0.049	—
2 M HCl (2)	1 st	0.992	0.114	—	1 st	0.987	0.344	—
H ₂ O (5)	2 nd	0.964	—	2.7	2 nd	0.999	—	2.2

k^1 – rate constant for 1st order reaction

k^2 – rate constant for 2nd order reaction

Except for alkaline leaching, the results indicated uniform trends in Fe stability; they proved the relative independence of Fe stability from the total Fe in initial samples, in contrast to strong dependence on the crystallinity of separate (oxyhydr)oxide Fe phases. Well crystallized phases (in KH and IH) were stable in acidic and water ionic and non-ionic environments, as evidenced by the different amounts of Fe released (see Table 2). Under alkaline conditions, no relation between Fe crystallinity and dissolution was found because of the stability of structural Fe(III) in alkaline solution, with possible destruction of Al and Si bonds in the clay mineral structure.

Structural changes in leached clays

The structural and surface changes of clay minerals that occurred during the leaching process were determined *via* equilibrium adsorption isotherms, thereby allowing description of appropriate fluctuations in porosity and specific surface area. The adsorption isotherms of well crystallized kaolinite (KH) and moderately crystallized bentonite (BCR) were measured before and after acidic and water leaching. The characteristic curves of pore-volume distribution obtained by the BJH method to nitrogen at 77 K (Figure 2), and the total porosity and S_{BET} (Table 4),

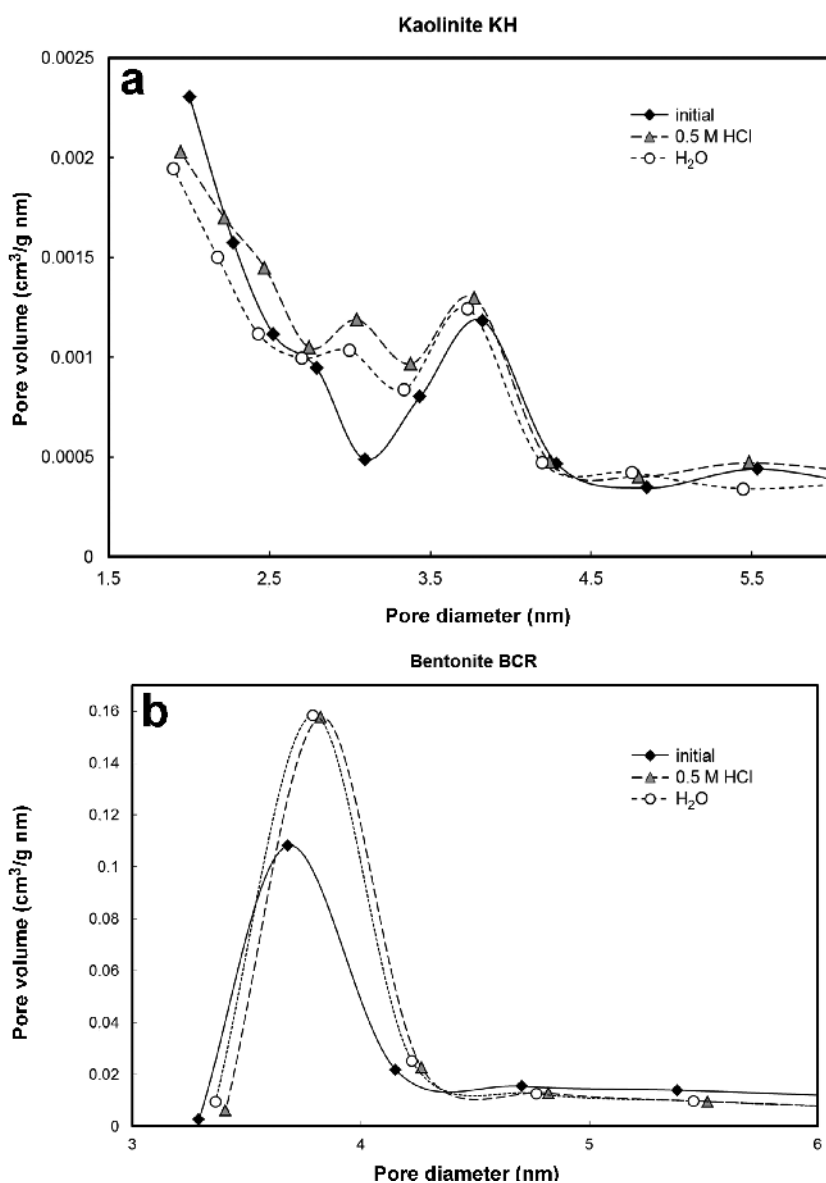


Figure 2. BJH pore-volume distribution of kaolinite KH (a) and bentonite BCR (b), leached for 24 h.

Table 4. Specific surface area and pore volume of initial and leached clay-mineral samples.

Sample	— Surface area, S_{BET} ($\text{m}^2 \text{g}^{-1}$) —			— Micropore volume $V_{\text{t-plot}}$ ($\text{cm}^3 \text{g}^{-1}$) —		
	Initial	0.5 M HCl	H_2O dist.	Initial	0.5 M HCl	H_2O dist.
Kaolinite, KH	5.59	6.69 (+19.7%)*	5.50 (−1.6%)	0.013	0.015 (+15.4%)	0.013 ($\pm 0\%$)
Bentonite, BCR	82.35	93.57 (+13.6%)	90.23 (+9.6%)	0.115	0.114 (−0.9%)	0.111 (−3.5%)

* relative difference from initial value

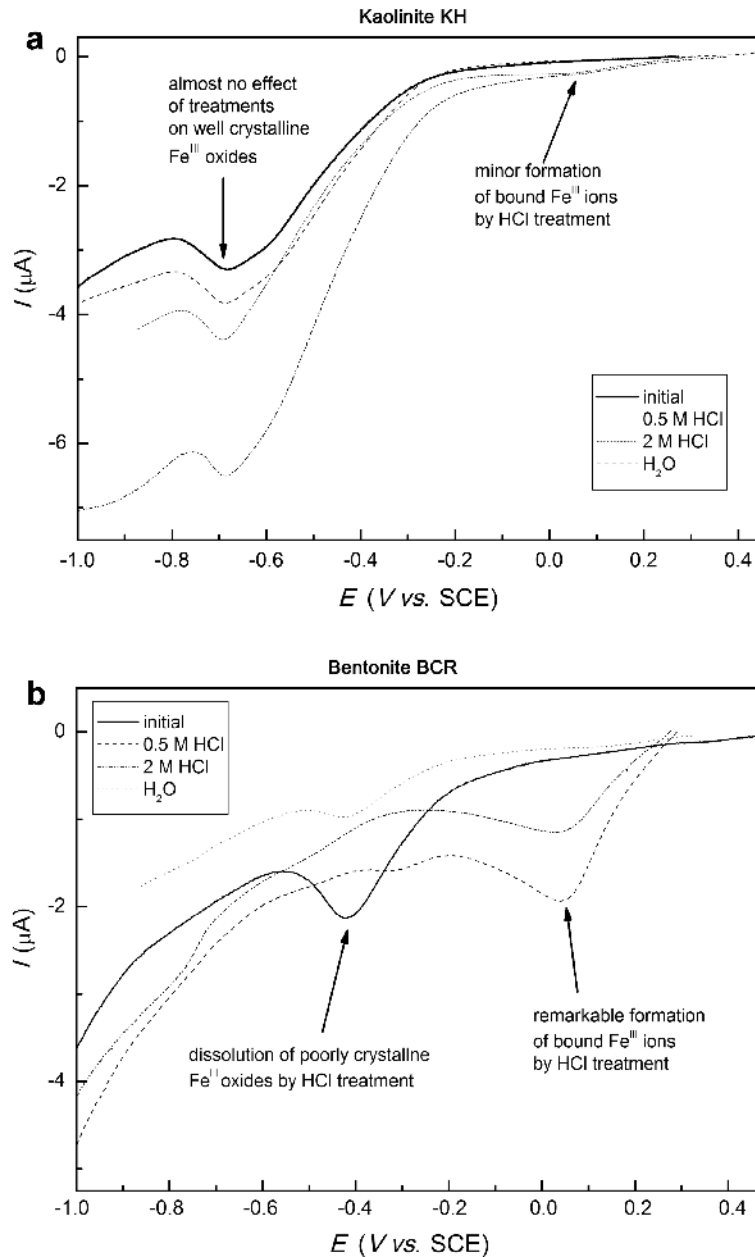


Figure 3. Voltammetric curves of kaolinite KH (a) and bentonite BCR (b) before and after acidic and aqueous leaching.

indicated that the bentonite has a relatively homogeneous pore structure, with the prevalent pore diameter being ~4 nm, whereas kaolinite pore space is more heterogeneous and of smaller diameters. The porosity in the bentonite is also larger than in the kaolinite. The variations in S_{BET} and pore volume observed during the leaching processes were not statistically significant, but indicated a direct correlation between the crystallinity and stability of Fe phases, leaching agent, and clay mineral type. The acidic leaching of kaolinite resulted in an apparent increase in S_{BET} and total micro-porosity, which denoted the formation of additional porosity at lower pore diameters (Figure 2a) (Lhotka *et al.*, 2012). The greater porosity and surface area after acidic leaching were probably caused by partial destruction of the kaolinite structure in the acidic environment. The distribution of porosity after neutral leaching of KH and BCR followed the acidic process (Figure 2a,b), but the data in Table 4 illustrate some changes compared to the acidic leaching. Water leaching did not modify the kaolinite structure. A greater mobility of Fe in bentonite (Table 2) resulted in a decline in micro-porosity due to the partial saturation of micropores with activated Fe^{3+} particles which were generated during the leaching process (Gil and Adamski, 2010).

Phase transformation of Fe due to the leaching process

Evaluation of equilibrium adsorption isotherms revealed changes in micro-porosity and surface area; voltammetry of microparticles can identify Fe phases in the clay structure, and give their oxidation state and phase transformations during the leaching process. This method was applied for quick and simple characterization of different HFO phases in clay minerals, alloys, and archeological objects (Cepriá *et al.*, 2003; Doménech *et al.*, 2013; Grygar *et al.*, 2002). As discussed above, kaolinite (KH) and bentonite (BCR) were chosen for comparison of their Fe characteristics via a voltammetric method. The voltammograms (Figure 3) showed possible variations in Fe phases during acidic and water leaching. According to Grygar *et al.* (2002) and van Oorschot *et al.* (2001), who identified small concentrations of Fe oxides in minerals, the peak at ~-0.75 V in Figure 3a can be assigned to well crystallized Fe(III) oxides in KH. This phase did not change markedly under the acidic leaching, but a partial chemical dissolution and phase transformation of Fe(III) microparticles may be indicated by the peaks at ~0 V (Figure 3a) (Cepriá *et al.*, 2003), which denoted the formation of reactive Fe^{3+} particles. Poorly crystallized Fe(III) oxides in BCR, which are characterized by the peak potential of -0.50 V (Figure 3b) (Cepriá *et al.*, 2003; Grygar *et al.*, 2002), were dissolved by acidic leaching. The process resulted in the remarkable formation of reactive Fe^{3+} particles as indicated by the prominent peaks at ~0.10 V. A similar run of initial and H_2O voltammetric curves (Figures 3a, 3b) illustrated

minor changes in Fe forms by water leaching. These results correspond well with those of Maqueda *et al.* (2008), who examined the behavior of Fe phases in untreated and acid-treated vermiculite. That study showed visible structural changes and a very small proportion of leached Fe in 0.25 M HCl.

CONCLUSIONS

The stability and phase transformations of structural Fe in clay minerals were mostly affected by the crystallinity of Fe particles. The total Fe and mineralogical characterization of clays were less important in leaching processes. Well crystallized Fe phases (60–90% of crystallinity) in kaolinite and illite were more stable in acidic, water ionic, and non-ionic environments compared to poorly crystallized Fe forms (20% to <50 % of crystalline Fe) in bentonite, kaolinite clay, and smectite clays ('red clays'). No relation between Fe crystallinity and mobility was observed under alkaline leaching due to Fe(III) stability in alkaline conditions. Micro-porosity and surface parameters related to leaching processes were affected markedly by the crystallinity of Fe particles; the changes in S_{BET} /pore volume in material with highly crystallized Fe related to a partial structural disturbance in acidic environment and were slightly affected by Fe changes. Materials containing less stable and poorly crystallized Fe forms demonstrated the participation of Fe released in the surface structure by the saturation of micropores with activated Fe^{3+} particles. Well crystallized Fe(III) oxides maintained their original structures with almost no effect by the leaching process. Poorly crystallized and amorphous Fe(III) phases were partially dissolved and transformed to much more mobile, ion-exchangeable Fe^{3+} ions forming active binding sites. The iron chemistry and phase transformation in clays influence their surface changes and adsorption properties.

ACKNOWLEDGMENTS

The authors acknowledge funding for the present study as part of project no. 13-24155S from the Grant Agency of the Czech Republic.

REFERENCES

- Alvarez Querol, M.C. (1952) Manganometric microtitration of iron. *Microchimica Acta*, **39**(2), 126–132.
- Barret, E.P., Joyer, L.G., and Halenda, P.P. (1951) The determination of pore volume and area distributions in porous substances. I. Computations from nitrogen isotherms. *Journal of the American Chemical Society*, **73**, 373–380.
- Bonnin, D., Miller, S., and Calas, G. (1982) Iron in kaolins: studies by EPR, Mössbauer, X-ray absorption, EXAFS. *Bulletin de Mineralogie*, **105**, 467–475.
- Brunauer, S., Emmet, P.H., and Teller, F. (1938) Adsorption of gases in multimolecular layers. *Journal of the American Chemical Society*, **60**, 309–319.
- Burleson, D.J. and Penn, R.L. (2006) Two-step growth of goethite from ferrihydrite. *Langmuir*, **22**, 402–409.

- Cepriá, G., Usón, A., Pérez-Arantegui, J., and Castillo, J.R. (2003) Identification of iron(III) oxides and hydroxy-oxides by voltammetry of immobilised microparticles. *Analytica Chimica Acta*, **477**, 157–168.
- Dávila-Jiménez, M.M., Elizade-González, M.P., Mattusch, J., Morgenstern, P., Pérez-Cruz, M.A., Reyes-Ortega, Y., Wennrich, R., and Hee-Madeira, H. (2008) In situ and ex situ study of the enhanced modification with iron of clinoptilolite-rich zeolitic tuff for arsenic sorption from aqueous solutions. *Journal of Colloid and Interface Science*, **322**, 527–536.
- Doménech, A., Lastras, M., Rodríguez, F., and Osete, L. (2013) Mapping of corrosion products of highly altered archeological iron using voltammetry of microparticles. *Microchemical Journal*, **106**, 41–50.
- Doušová, B., Fuitová, L., Grygar, T., Machovič, V., Koloušek, D., Herzogová, L., and Lhotka, M. (2009) Modified aluminosilicates as low-cost sorbents of As(III) from anoxic groundwater. *Journal of Hazardous Materials*, **165**, 134–140.
- Doušová, B., Lhotka, M., Grygar, T., Machovič, V., and Herzogová, L. (2011) In situ co-adsorption of arsenic and iron/manganese ions on raw clays. *Applied Clay Science*, **54**, 166–171.
- Favre, F., Bogdal, C., Gavillet, S., and Stucki, J.W. (2006) Changes in the CEC of a soil smectite-kaolinite clay fraction as induced by structural iron reduction and iron coatings dissolution. *Applied Clay Science*, **34**, 95–104.
- Ferris, A.P. and Jepson, W.B. (1975) The exchange capacities of kaolinite and the preparation of homoionic clays. *Journal of Colloid and Interface Science*, **51**, 245–259.
- Gil, B. and Adamski, A. (2010) Complementary use of IR and EPR spectroscopies for characterization of iron species in thermally treated MFI-type zeolites. *Microporous and Mesoporous Materials*, **127**, 82–89.
- Grygar, T., Bezdička, P., Hradil, D., Doménech-Carbó, A., Marken, F., Pikna, L., and Cepriá, G. (2002) Voltammetric analysis of iron oxide pigments. *Analyst*, **127**, 1100.
- Grygar, T., Hradil, D., Bezdička, P., Doušová, B., Čapek, L., and Schneeweiss, O. (2007) Fe(III) modified montmorillonite and bentonite: Synthesis, chemical and UV-VIS spectral characterization, arsenic sorption, and catalysis of oxidative dehydrogenation of propane. *Clays and Clay Minerals*, **55**, 165–176.
- Hassan, M.S. and Salem, S.M. (2002) Distribution and influence of iron phases on the physico-chemical properties of phyllosilicates. *Chinese Journal of Geochemistry*, **21**, 29–39.
- Izumi, Y., Masih, D., Aika, K., and Seida, Y. (2005) Characterization of intercalated iron(III) nanoparticles and oxidative adsorption of arsenite on them monitored by X-ray absorption fine structure combined with fluorescence spectrometry. *The Journal of Physical Chemistry B*, **109**, 3227–3232.
- Komadel, P., Madejová, J., and Stucki, J.W. (2006) Structural Fe(III) reduction in smectites. *Applied Clay Science*, **34**, 88–94.
- Lhotka, M., Machovič, V., and Doušová, B. (2012) Preparation of modified sorbents from rehydrated clay minerals. *Clay Minerals*, **47**, 251–258.
- Malat, M. (1973) *Absorption Inorganic Photometry*. Academia, Prague (in Czech), pp. 684–709.
- Madejová, J., Pentrák, M., Pálková, H., and Komadel, P. (2009) Near-infrared spectroscopy: A powerful tool in studies of acid-treated clay minerals. *Vibrational Spectroscopy*, **49**, 211–218.
- Manceau, A., Drits, V.A., Lanson, B., Chateigner, D., Wu, J., Huo, D., Gates, W.P., and Stucki, J.W. (2000) Oxidation-reduction mechanism of iron in dioctahedral smectites: 2. Crystal chemistry of reduced Garfield nontronite. *American Mineralogist*, **85**, 153–172.
- Maqueda, C., Santas Romero, A., Morillo, E., Pérez-Rodríguez, J.L., Lerf, A., and Wagner, F.E. (2008) The behavior of Fe in ground and acid-treated vermiculite from Santa Olalla, Spain. *Clays and Clay Minerals*, **56**, 380–388.
- Pentráková, L., Su, K., Pentrák, M., and Stucki, W. (2013) A review of microbial redox interactions with structural Fe in clay minerals. *Clay Minerals*, **48**, 543–560.
- Sei, J., Jumas, J.C., Olivier-Fourcade, J., Quiquampoix, H., and Staunton, S. (2002) Role of iron oxides in the phosphate adsorption properties of kaolinites from the Ivory Coast. *Clays and Clay Minerals*, **50**, 217–222.
- Stucki, J.W., Goodman, B.A., and Schwertmann, U. (1988) *Iron in Soils and Clay Minerals*, pp. 447–480, 625–642. D. Riedel Publishing Company, Dordrecht, The Netherlands.
- Sultana, U.K., Gulshan, F., and Kurny, A.S.W. (2014) Kinetics of leaching of iron oxide in clay in oxalic acid and hydrochloric acid solutions. *Materials Science and Metallurgy Engineering*, **2**, 5–10.
- van Oorschot, I.H.M., Grygar, T., and Dekkers, M.J. (2001) Detection of low concentrations of fine-grained iron oxides by voltammetry of microparticles. *Earth and Planetary Science Letters*, **193**, 631–642.
- Webb, P.A. and Orr, C. (1997) *Analytical Methods in Fine Particle Technology*. Micromeritics Instrument Corporation, Norcross, Georgia, USA.
- Yang, L., Donahoe, R.J., and Redwine, J.C. (2007) In situ chemical fixation of arsenic contaminated soils: An experimental study. *Science of the Total Environment*, **387**, 28–41.
- Žák, T. and Jirásková, Y. (2006) CONFIT: Mössbauer spectra fitting program. *Surface and Interface Analysis*, **38**, 710–714.

(Received 2 January 2014; revised 26 May 2014; Ms. 832; AE: J. Miehé-Brendlé)